ISSN Online: 2709-7625
ISSN Print: 2709-7617
Vol.7 No.3, 2024

Structural and Magnetic Properties of Co_2FeAl Full Heusler Alloys synthesized by Hydrothermal Method

Abdul Basit
maharbasit99@gmail.com
University of the Punjab Lahore
Muhammad Yaseen
my996627@gmail.com
University of the Punjab Lahore
Saira Riaz
saira.cssp@pu.edu.pk
University of the Punjab

ABSTRACT

Full heusler alloys have attracted the attention of research community owing to its potential applications in spintronic devices. Hydrothermal technique is used to prepare Co_2FeAl full Heusler alloys. Molarity of the electrolytes is varied as 1.2M, 1.4M, 1.6M, 1.8M & 2.0M. The prepared Co_2FeAl full Heusler alloys nanoparticles are characterized by XRD, VSM, FTIR and hall measurements. Mixed phases of Co_2FeAl - hexagonal and CoAl-tetragonal are observed for the samples having molarity ranging from 1.2M to 1.6M. Whereas, pure Co_2FeAl hexagonal phase is attained for the samples prepared with 1.8M & 2.0M solutions. FTIR (Fourier transform infrared spectra) is recorded for the Co_2FeAl based full-heuslar alloy nanoparticles with varying molarity ranging from (1.2M-2.0M) that is done in the range of mid IR (300-500 cm-1). FTIR analyzes structural & chemical changes due to different functional-groups. Magnetic analysis of Co_2FeAl based full-heuslar alloy nanoparticles shows the soft ferromagnetic behavior for all the samples. Current-voltage (I- V) characteristics are measured for the variation in molarities. Temperature dependent Current-voltage (I-V) characteristics are measured for the samples with pure Co_2FeAl full heuslar alloy structure i.e. sample prepared with 2.0 M solution

1 Introduction

The basic introductory chapter consists of Heusler alloys, their structure and importance. On behalf of properties of the solids, their various structural types, magnetic ability and band gaps have been found. A brief discussion about the properties of Heusler alloys and Heusler compounds is discussed in this chapter.

A nanoparticle or as well as ultrafine particle are commonly known, matter particle with such a diameter between 1 and 100 nanometers (nm). The progress from miniature particles to nanoparticles can prompt various changes in actual properties. Two of the main considerations in this are expansion in the proportion of surface region to volume, and size of the molecule moving into the domain where quantum impacts prevail.

The huge surface space of nanoparticles likewise results I n a great deal of communications between the intermixed materials in nanocomposites, prompting unique properties like expanded strength and additionally expanded compound/heat obstruction.

Significance of Nanoparticles

The most significant of these incorporate the utilization of nanoparticles in (1) drug conveyance, (2) tissue recovery and (3) demonstrative/imaging applications. The properties of nanoparticles in medication advance and work with fast cell take-up.

Everyday products that are use nanotechnology

1. Clothing
2. Furniture
3. Adhesive
4. Coatings for car paintwork
5. Tennis ball

6. computers

Heusler alloy

Heusler combination any of first attractive compounds made out of metals that in their unadulterated state, are not attractive. Composites are named after Fritz Heusler nineteenth century German mining specialist and scientist. Heusler amalgams comprises of around two pieces of copper, one of magnese and one of Tin. The Tin might be supplanted by aluminum, arsenic, antimony, bismuth, or boron, the copper might be supplanted by silver.

The disclosure of these composites didn't draw in much consideration in England until 1904, when R.N. Hadfield showed an example at the gathering of British Association, and soon a short time later Fleming and Hadfield distributed aftereffects of their examination. Due to theoretical and experimental concentration, Heusler alloy has these unique properties

- Half –metallic behavior
- Magnetic shape memory effect
- Inverse magnetocaloric effect

In 1983 de Groot and his callaboraters were the first who introduced the half-metallicity. At the point when they were examining the band construction of half-Heusler combination Ni-Mn-Sb. The half-metallic ferromagnets are the most well-known material for examining to talk about. In the minority-spin band structure the existing gap causes about 100% spin polarization at the Fermi level of the electrons which would lead the emerging field of spintronics. In the half- metals it should be possible for the spin-polarized current if the efficiency of magneto-caloric devices is increased. But the change carriers in ground state will create a strong spin polarization.

2 Literature Review

This work reports the attractive and electronic portrayal of plane charged covered Heusler Co2FeAl nano slight movies of various thickness by X-beam retentions spectroscopy (XAS) and X-beam attractive roundabout dichroism (XMCD) estimations. . The spectra on both Co and Fe L2,3 edges show an articulated attractive dichroic signal in remanence, relating to a ferromagnetically-adjusted minute on Fe and Co particles molding the impossible to miss qualities of the Co2FeAl Heusler compound (a half-metallic ferromagnet). The definite information on the connected attractive and electronic properties of these examples over a wide scope of thickness of movies are basic for accomplishing a higher passage magnetoresistance proportion, and in this way for spintronics gadget applications.[7]

Previous Research on Heusler Alloys

Ortiz et al., (2011) revealed an underlying and attractive investigation of two Co2FeAl tests; one with Cr cradle and the other with MgO support. XRD and RHEED showed that the two examples were epitaxialy filled in the B2B2 stage. Apparently Cr cradle gives a superior translucent quality, as confirmed by XRD, bigger immersion polarization, and lower damping factor. Notwithstanding, this example presents a bigger extraneous linewidth, demonstrating the presence of a greater number of inhomogeneities than for the MgO cushioned one [8].

Gabor et al., (2015) organized Co2FeAl films of various thicknesses (10 nm≤d≤100 nm) by wavering on Si(001) substrates and hardened at 600 °C. XRD assessments revealed an (011) out-of-plane completed advancement of the motion pictures with no in-plane specific improvement bearing. The matrix limit increases with growing CFA thickness, apparently in light of the improvement of the substance demand. MOKE hysteresis circles obtained with different field headings uncovered that the straightforward center point coercive field changes straightly with the regressive CFA thickness. The microstrip ferromagnetic resonation has been used to think about the incredible properties. The jaunty and the field states of the resonation field and repeat, exclusively, have been analyzed through a model ward on an alluring energy

thickness which, regardless Zeeman, demagnetizing and exchange terms, is portrayed by a uniaxial choose the main limits. The in-plane uniaxial anisotropy field, present in all of the models, increases straightly with the regressive CFA thickness. The reasonable charge shows fundamentally straight addition with the inverse CFA thickness suggested

surface anisotropy affected by the CFA/MgO interface However, the uniaxial anisotropy basic center point bearing changes with the thickness [9].

Half-metallic ferromagnets (HMFs), which were first anticipated in Heusler compounds by Groot et al., (1951) pulled in impressive consideration because of their possible application as an exceptionally turn energized current source in spintronics gadgets. As announced in writing, Co2FeAl had three crystallographic structures: A2, B2 and L21. In this work, Co2FeAl Heusler compound nanoparticles were blended by coprecipitation and warm deoxidization strategy. The examinations through X-beam diffraction transmission electron microscopy, vibrating test magnetometry and Mössbauer spectroscopy all uncovered unambiguously B2 structure and similar stoichiometry of Co2FeAl particles contrasted and the circular segment liquefying and the mechanical alloying strategy. In this way, the coprecipitation and warm deoxidization strategy could be a proficient method to get Heusler composite nanoparticles [10].

Okamura et al., (2005) investigated the essential properties of Co2FeAl s100 nm thicked films, TMR in Co2FeAl/Al–Ox/Co75Fe25 MTJs, and the oxidizations at the surfaces of Co2FeAl films and the interfaces in MTJs. They won concerning setting up the A2 and B2 type jumbled Co2FeAl films by saving at room temperature and temperatures higher than 473 K, independently. A biggest TMR of 47.3% at RT is gotten in the MTJs with a Co2FeAl hardened in the A2 structure, which is credited to the clean sno oxidizedd Co2FeAl surface. Regardless, MTJs with the B2 type jumbled Co2FeAl kept at 573 K have shown recently 27% TMR. These TMR results are dependable with the calculation of the bend polarization for Co2FeAl with the different issues [11].

Zhao et al., (2013) orchestrated the essential and alluring properties of a movement of Co2FeAl Heusler compound films become on GaAs (001) substrate by sub-nuclear column epitaxy have been analyzed. The epitaxial Co2FeAl films with an organized L21 structure have been successfully gotten at improvement temperature of 433 K, with an in-plane cubic appealing anisotropy superimposed with a phenomenal uniaxial alluring anisotropy. With extending improvement temperature, the organized L21 structure adulterates. Meanwhile, the uniaxial anisotropy decreases and over the long haul evaporates above 673 K. The interfacial holding among As and Fe or Co particle is prescribed to be obligated for the extra uniaxial anisotropy [12].

Zhang et al., (2018) were effectively combined nuclear scale attraction of Co2FeAl Heusler compounds with the thickness down to the nanometer scale, this turns out to be considerably more modern. A basic thickness of 3 uc has been recognized, beneath which an enemy of equal twist part of the Co particles happens. This enemy of equal twist part can be liable for the fundamentally diminished attractive second and the low spinpolarization close to the Fermi level of the Co2FeAl. Solid uniaxial attractive anisotropy has been seen from all thicknesses of the Co2FeAl slight movies between 3unit cells (uc) and 20 uc. A basic thickness of 3 uc has been distinguished, underneath which an enemy of equal twist part of the Co molecules happens [13].

Petrisor et al., (2011) Co2FeAl arranged Co2FeAl movies of different thicknesses (10 nm≤d≤100 nm) by faltering on Si(001) substrates and toughened at 600 °C. XRD estimations uncovered an (011) out-of-plane finished development of the movies with no in-plane particular development direction. The grid boundary increments with expanding CFA thickness, likely because of the upgrade of the substance request. The in-plane uniaxial

anisotropy field, present in every one of the examples, increments directly with the backwards CFA thickness. Notwithstanding, the uniaxial anisotropy simple hub course changes with the thickness. The powerful polarization shows definitely direct increment with the converse CFA thickness proposing a surface anisotropy initiated by the CFA/MgO interface. MOKE hysteresis circles acquired with various field directions uncovered that the simple pivot coercive field changes straightly with the opposite CFA thickness. The microstrip ferromagnetic reverberation has been utilized to consider the powerful properties. The precise and the field conditions of the reverberation field and recurrence, separately, have been examined through a model dependent on an attractive energy thickness which, notwithstanding Zeeman, demagnetizing and trade terms, is described by a uniaxial anisotropy to decide the most significant boundaries [14].

Zhang et al., (2008) considered the underlying and attractive properties of Co2FeAl films become on GaAs (001) substrates at various temperatures. It is tracked down that the single-gem Co2FeAl dainty movies with level of L21 request could be gotten on GaAs (001) substrates by MBE. The enormous increment of the coercivity Hc for [110] bearing at high development temperatures is proposed to result from the impressive hybridization of states among Co and Fe particles. Also, the uniaxial anisotropy diminishes with expanding development temperature and totally vanishes above 673 K. Our exploratory examinations give helpful knowledge to understanding the beginning of the uniaxial anisotropy of epitaxial Co2FeAl slim movies, and better designing of the anisotropy for potential Co2FeAl-based spintronics applications. The in-plane uniaxial anisotropy is proposed to be basically identified with the awry interfacial holding among As and Co or Fe [15].

Sharma et al., (2016) added to a superior comprehension of the starting points of epitaxial Co2FeAl dainty film uniaxial anisotropy, just as better designing of the anisotropy for planned Co2FeAl-based spintronics applications. Our examination added to a superior comprehension of the beginnings of epitaxial Co2FeAl slight film uniaxial anisotropy and better designing of the anode. Our XMCD spectra show that there is an equal arrangement of Fe turns, which implies that no nuclear cluttering exists in our example. Because of this explanation the complete attractive snapshot of Fe at L2,3 edges increments with the thickness of the Co2FeAl meager film. From XMCD they likewise tracked down an unmistakable ferromagnetic sign at Co site and the information obviously show that Fe and Co are ferromagnetically adjusted for all film [16].

Kumar et al., (2016) Mechanical alloying (MA) has been utilized to create the Co2FeAl Heusler compound with a nanocrystalline structure. The development instrument of the amalgam researched. Rietveld examination showed that every one of the examples that were processed for >15 h had a L21 structure with a space gathering of Fm3m. The crystallite size and inward strain of the examples were determined utilizing the Williamson–Hall condition. The crystallite size of Co2FeAl expanded to ∼22 nm by expanding the MA time from 14 to 22 h, and after 22 of MA, the crystallite size diminished. Interestingly, the interior strain has expanded with the increment in processing time. The powder acquired after 20 h of MA was parted into three sections and independently tempered at 300, 500 and 700°C for 5 h. An extensive increment was seen in the hardness worth of powder particles with the increment in toughening temperature up to 500°C. Notwithstanding, the hardness worth of the example strengthened at 700°C diminished. It appears to be that this component is identified with boundaries, for example, expansion in crystallite size, upgrade of cross section requesting, change in thickness of imperfections and pollutions and non-stoichiometer impacts [17].

Dalela et al., (2016) in this report, the combination and portrayal of Heusler compound Co2FeAl nanoparticles have been illustrated. XRD and SAED results affirm the development of CFA compound stages (L21, B2 and A2). TEM examination shows the development of

nanoparticles size going from 10 nm to 50 nm which is in acceptable concurrence with crystallite size. The polarization conduct of CFA nanoparticles shows ferromagnetic conduct at room temperature with an immersion charge of 115 emu/g, which is near mass worth of CFA compound as announced by Slater-Pauling bend [18].

Husain et al., (2017) a nitty gritty investigation of the impact of two various types of warm handling treatment viz, post development toughening and higher substrate temperature during development (series 'A' and series 'S' separately), on the charge dynamical properties of particle pillar faltered Co2FeAl slender movies saved on Si (100) was performed. A connection among the primary, static and dynamic polarization reaction of these Co2FeAl films is set up vis-a-viz the warm treatment during film-testimony and post-statement however in situ as it were. Specifically, impacts of both the warm medicines were looked at on two series of Co2FeAl films. The movies were polycrystalline in nature with close to ideal stoichiometry (nuclear proportion of Co and Fe is practically steady ~ 2) and moderate immersion charge (~900 kA/m). The examination uncovered that fundamentally, the Co2FeAl films with post strengthening are better with higher thickness (6.36 ± 0.09 g/cm3) and lower interface unpleasantness (0.48 ± 0.03 nm) contrasted with the movies developed at higher substrate temperature (6.23 ± 0.06 g/cm3, 0.61 ± 0.01 nm). The immersion polarization of the Co2FeAl films developed at higher substrate temperatures are somewhat higher contrasted with that found in the post toughened movies. In plane field-point subordinate longitudinal magneto optical Kerr impact study uncovered that attractive anisotropy of these movies has synchronous uniaxial and biaxial commitments [19].3 Experimental Tools

Material sciences evolve many methods for synthesis and characterization of the material. These methods are of great importance according to need and requirement. These methods are different in many ways like cost, environmental hazards, quality of product etc. At the same time characterization of material involve many factors to reveal about the material. There are many ways to reveal the hidden truths about the composition, crystal structures, topology, morphology etc. In this chapter a brief introduction of different methods of synthesis and characterization is under discussion.

Experimental techniques are one of the major part of a research work. These plays an important part by giving us experiment evidences of our work. Following are the significant part of the experiments for the characterization of the specific material.

Electronic balance is an instrument which is easy and quick way for weighing samples and materials. The least count of electronic balance is 0.01 mg. It is very important part of experiment. This is not only the accurate way but also not to expensive. This device is used to find accurate measurements of weight shown in fig. 1.3. [20]

Figure 3.1 Electronic Balance

3.1.1 Hot plate and magnetic stirrer

ISSN Online: 2709-7625
ISSN Print: 2709-7617
Vol.7 No.3, 2024

This device is used to make a stir bar, immerse in a liquid, quickly, spin, or stirring or mixing a solution. SHMS wise stir- digital Magnetic stirrer is a good experimental apparatus for drying and heating up the sample. It is very easy to handle and has fast start up. Hot plate has temperature tendency upto 350 c ˚. Magnetic stirrer can stir speed of 80-1500 rpm. Fig. 3.2 represents hot plate.

3.1.2 Autoclave

3.1.3 Figure 3.2 Hot Plate and magnetic stirrer

An autoclave is utilized in clinical and lab settings to disinfect lab hardware and waste. Autoclave sanitization works by utilizing warmth to kill microorganism like microscopic organisms and spores. Its nontoxic and economical, it kills microorganisms and spores quickly and rapidly heat and enters textures. Autoclave comes in different versions. There varieties come according to the materials. The walls of the autoclave are very important and its needs lining of specific materials to avoid corrosion. Teflon lining is required to avoid corrosion inside the vessel. Teflon lining decreases or mostly remove the chance of cracking or damaging of walls. Autoclave has mainly two varieties and PTFE polytetrafluoroehtylene or it is called Teflon lined autoclave. PTFE is made up of highly quality stainless steel and inside its chamber is lined with Teflon. Temperature and pressure are two parameters and their limits decide the variety of the autoclave. First one autoclave is Teflon lined autoclave and it has 240˚c maximum limit for temperatures while the safe temperatures limit for this type is 200˚c. While second case maximum limit for temperature is higher than PTFE. It can
work on higher temperature and maximum limit for PPL lined autoclave is 280˚c. While the safe temperature for this type is 260˚c [21]. Fig. 3.3 represents autoclave.

ISSN Online: 2709-7625
ISSN Print: 2709-7617
Vol.7 No.3, 2024

3.1.4 Furnace Box

Figure 3.3 Autoclave

A container heater an upward lift or swing out entryway permitting the different estimated items to be put in the heater. Box heaters are used for heat-treating, treating, relieving, preheating and other high temperature warm interaction. Box heaters are regularly utilized in a wide scope of warming interaction. Its provisions an entryway and it composites sizes to be put inside the heater. Temperature sign and screen is available underneath the. Box heaters comes distinctive model with vertical or even entryway opening to present day and better methodology displayed in fig. 3.4. [22]

ISSN Online: 2709-7625
ISSN Print: 2709-7617
Vol.7 No.3, 2024

3.1.5 Fume hood

3.1.6 Figure 3.4 Furnace Box

A smoke hood is a ventilated fenced in area wherein gases, fumes a lot are contained. An exhaust fan arranged on the highest point of the research facility structures gets air and airborne impurities through associated ventilation work and exhaust them to the air. In spite of the fact that smoke hoods are fundamental they can't secure against each research facility danger. Very risky work will require explicitly planned hardware. Smoke hoods are significantly more productive and viable strategy for containing risky materials than a piece of individual defensive hardware, for example, a breath addresses in fig. 3.5. [23]

ISSN Online: 2709-7625
ISSN Print: 2709-7617
Vol.7 No.3, 2024

3.1.7 Centrifuge

Figure 3.5 Fume Hood

A machine with a quickly pivoting holder that applies outward power to its substance, normally to isolate liquids of various densities (e.g cream from milk) or fluids from solids. It is utilized to isolate particles suspended in a fluid as per molecule size and thickness, consistency of the medium, and rotor speed. Inside an answer, gravitational power will make particles of higher thickness than the dissolvable sink, and those less thick than the

dissolvable to buoy to the top displayed in fig. 3.6.[24]

Figure 3.6 Centrifuge

3.2 Sample preparation

Sample preparation is very important in any research work. For this particular research work, hydrothermal method is type of solvent synthesis and is used to prepare materials for many purposes.

3.2.1 Hydrothermal Method

"Hydro" implies water and "Warm" implies heat. It is a synthetic response in water is fixed pressing factor vessel which is truth a sort of response at high temperature and pressing factor. It is a famous synthesis techniques among scientist. The term hydrothermal is geologic origion. Hydrothermal method is also a source of producing crystals artificially and naturally at the same time. Minerals are natural product of hydrothermal process. Many scientist also claimed that they make crystals or artificial diamond by using hydrothermal techniques. Temperature and pressure are two major parameters and they mutually set conditions for hydrothermal process. This reaction usually needs to proceed at above 100˚c and one bar [25]
Important parts of hydrothermal synthesis

- Autoclave
- Reaction solvent
- Magnetic heater and stirrer
- Digital indicator
- Temperature indicator or thermometer

3.2.2 Water as a reaction medium

Water is a universal solvent. It is abundant in nature and easily available. Most of the element dissolve in at room temperature. Some dissolve at specific temperature water has unique physical and chemical properties. It is low cost and favourite reaction medium for many process. Water is environment friendly and it can be removed from the product as it is volatile in nature. Water has too many works to do. It is a catalyst and at the same time works as reactant and somewhere is will be a solvent and then a cooling agent and much more. It is also non-toxic.
Advantages of hydrothermal method are:

1. Mild operating conditions
2. One step synthetic procedure
3. Environmental friendliness
4. Inexpensive
5. Good dispersion in solution

3.3 Characterization Techniques

Different experimental techniques are used to evaluate results after using experimental method. Experimental methods give us products that are desired. Now first step is making or producing product by using different methods. Second step is to check and make a conclusion about it by different experimental techniques. These techniques use different machines to analyze the product made by experimental methods.
Conclusion made under the observation find by the experimental methods or procedure predicts many things for future. These results are valuable to give a material or product a standard quality, advantages, hazards and how to use and where to. This also predict the best method to make good quality product or the cheapest and safe way to produce it. Different experimental techniques are available in market and laboratory. These techniques vary with need and the product or material that is available for experimenting [26]

3.3.1 X-ray Diffractometer (XRD

A diffractometer is an estimating instrument for breaking down the design of a material from the dissipating design created when a light emission or particles interfaces with it. X beam diffraction, often contracted as XRD, is a non-damaging test strategy used to investigate the construction of glasslike materials. XRD examination, via the investigation of the gem structure, is utilized to distinguish the glasslike stages present in a material and along these lines uncover synthetic creation data. Bragg law, in physical science, the connection between the dispersing of nuclear planes in precious stones and the points of rate at which these planes produce the most extreme impressions of electromagnetic radiations, for example, X beams and gamma beams, and molecule waves, for example, those related with electrons and neutrons. Bragg's law states that a plane wave diffracted by a collection of cross segment planes must satisfy the following conditions: 2 d sin = n, where d is the interplanar isolating point between the wave vector of the scene plane wave, ko, and the lattice planes, its recurrence, and n is an entire integer, the reflection solicitation Diffraction Methods of X-RAY diffraction
X-ray diffraction consists of three types

1. Laue’s method
2. Rotating crystal method
3. Powder method

3.3.1.1 Laue’s Method

ISSN Online: 2709-7625
ISSN Print: 2709-7617
Vol.7 No.3, 2024

Laue diffraction in X-rays, a customary exhibit of spots on a visual emulsion coming about because of X-beams dissipated by specific gatherings of equal nuclear planes inside a precious stone. Laue diffraction, first identified by Max von Laue, a German physicist, is significant for gem investigation. The Laue technique is principally used to decide the direction of huge single precious stones. White radiation is reflected from, or communicated through, a proper gem. The diffracted radiates structure varieties of spots, that lie on bends on the film. The Bragg point is fixed for each set of planes in the gem

3.1.2.3 Variation of Laue's Method

Laue's method exhibited two variations by changing the relative position of source crystal and film. Transmission Laue's method in this method film is placed behind the crystal and the diffracted beams are transmitted partially through the crystal and the films the record the beam in forward direction.

Back reflection Laue's method in this particular variation film is placed between the x ray source and the crystal. The film has a hole and the incident beam passed through it and the diffracted beam is recorded in the backward direction.

3.1.2.3 Rotating crystal Method

A single gem is attached with one of its pivots in this approach, which is typical of monochromatic light emission beams. The precious stone is encased in a tube-shaped coating. With these conditions, the gem is rotated, and the precious stone's pivot of rotation harmonises with the film's centre. Rotation of crystal performs under chosen directions. Only a particular set of lattice planes satisfies the Bragg's condition and make the correct angle for x-ray reflection. A reflected beam formed and one can determine the unknown crystal structure [27]. Rotating crytal method is shown in fig. 3.7.

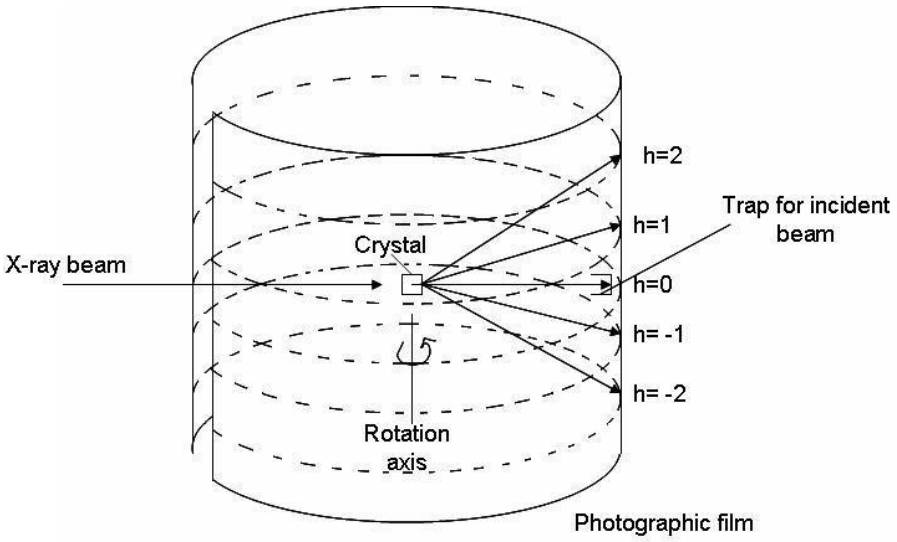

Figure 3.7 Rotating crystal

3.4.1.4 Powder method

ISSN Online: 2709-7625
ISSN Print: 2709-7617
Vol.7 No.3, 2024

The main difference powder and other is that method is that powder method uses poly crystal which is in the powder form. Monochromatic beam x-ray is used with variable angle however lambda fixed in this case. This method is useful in finding the lattice parameters which are magnitudes of the unit vectors symbolized as a, b, c. Unit cell can be defined in terms of these unit vectors. In case of single crystal only one or two diffracted beams will be formed [28]. Fig. 3.8 represents powder method.

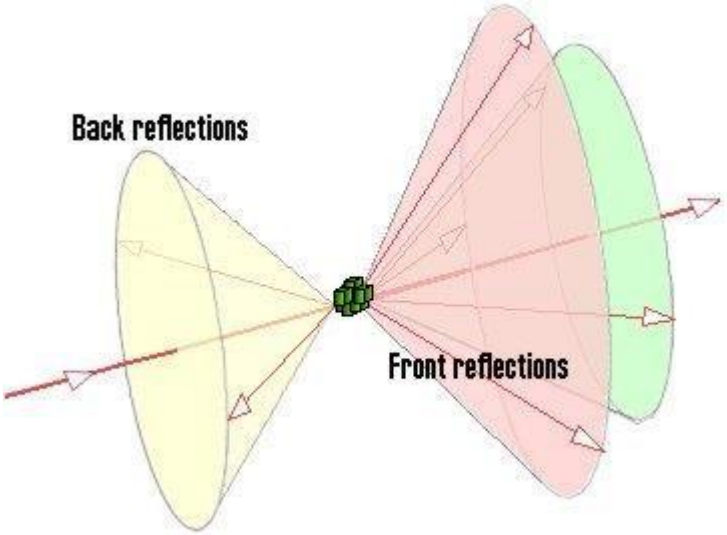

Figure 3.8 powder method

3.4.4 Vibrating sample magnetometer (VSM)

A vibrating test magnetometer (VSM) deals with Faraday's Law of Induction, which reveals to us that a changing appealing field will make an electric field. This electric field can be assessed and can reveal to us information about the changing alluring field. A VSM is used to measure the alluring behavior of appealing materials. A VSM works by first setting the guide to be amassed in a consistent alluring field. If the model is appealing, this predictable alluring field will charge the model by changing the appealing regions, or the individual alluring turns, with the field. The more grounded the consistent field, the greater [29]. The advancement of

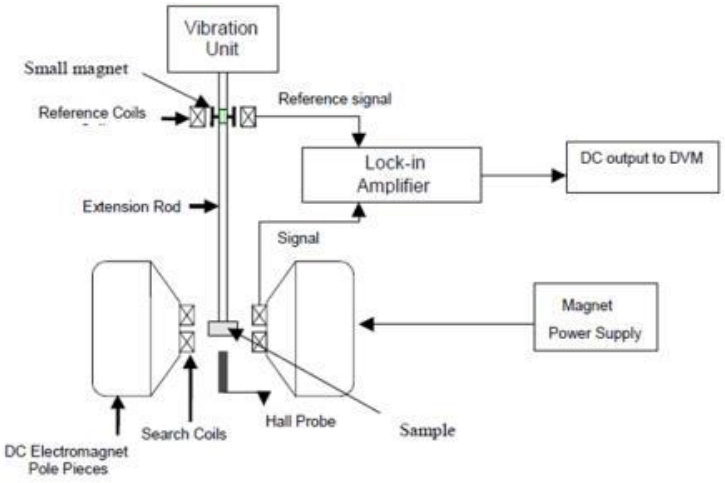

VSM is shown in fig. 3.9.

ISSN Online: 2709-7625
ISSN Print: 2709-7617
Vol.7 No.3, 2024

Figue 3.9 VSM

3.4.5 FTIR Analysis

FTIR measures the vibration and rotation of molecules which can provide information about the nature of their interactions. IR stands for 'Infrared' which ranges from 0.8-2.5 μm wavelength in the electromagnetic spectrum. FTIR is widely used because it can produce an interferogram in within a second. An interferogram is a complex pattern that contains all the infrared frequencies. FTIR spectrometer simultaneously accumulates high-extraordinary objective data over a wide apparition reach. The term Fourier-change infrared spectroscopy starts from the way that a Fourier change (a mathematical cycle) is expected to change over the unrefined data into the genuine reach [30]. FTIR spectroscopy is shown in fig. 3.10.

Figure 3.10 FTIR Analysis

3.4.6 Hall Measurements

The Hall impact is the creation of a voltage contrast across an electrical transmitter that is cross over to an electric flow in the conveyor and to an applied attractive field opposite to the flow. It was found by Edwin Hall in 1879.

A Hall impact can likewise happen across a void or opening in a semiconductor or metal plate, when current is infused through contacts that lie on the limit or edge of the void or opening, and the charge streams outside the void or opening, in the metal or semiconductor. This Hall impact becomes detectable in an opposite applied attractive field across voltage contacts that lie on the limit of the void on one or the other side of a line interfacing the

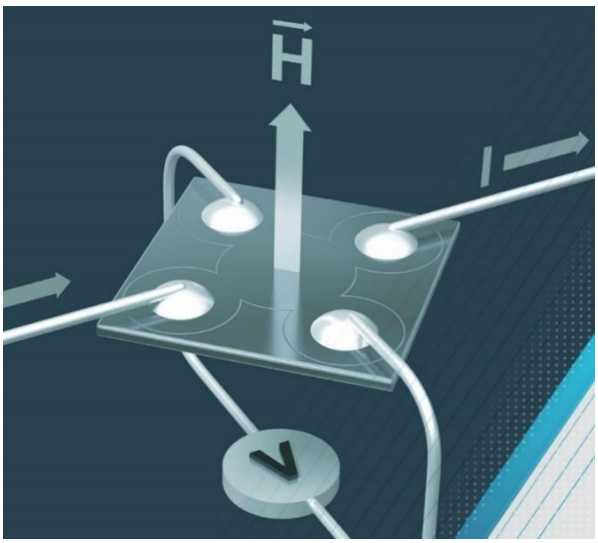

Figure 3.11 Hall Measurements

current reaches, it shows obvious sign inversion in contrast with the standard common Hall impact in the just associated example, and this Hall impact relies just upon the current infused from inside the void [31]. Fig. 3.11 delineates aqueous arrangement.

Chapter 4 Results and Discussions

4.1 Introduction

Co_2FeAl full heuslar alloys are synthesized byvarying molarities (1.2M to 2.0M) via hydrothermal method. The obtained nanoparticles are then characterized. To evaluate the properties of these nanoparticles, different techniques were used. X-ray diffraction (XRD) technique was used for the structural analysis. For magnetic analysis vibrating sample magnetometer (VSM) was used. IV measurements are carried out by using Hall measurements. Results for all the techniques are discussed below in detail.

4.2 Structural Analysis

Fig 4.1 shows the XRD patterns of Co_2FeAl full-heuslar alloy with varying molarity from 1.2M to 2.0M. All the planes (102), (104), (110), (201), (202), (204), (205), (214) and (300) of electrodeposited Co_2FeAl full-heuslar alloy exhibited hexagonal structure having space group P63/mmc. For all molarities the preferred orientation is along (110) plane. Mixed phases were observed at low molarities while phase pure Co_2FeAl was observed at high molarities i.e. at 1.2M to 2.0M. Due to internal stresses and minimization of surface energy, crystallites preferential growth along certain plane occurs. Phase change was observed with increasing molarity at 1.8M from mixed phase to pure phase. Further increase in molarity upto 2.0M only phase stability and strengthening of Co_2FeAl based full-Heuslar alloy hydrothermally deposited nanoparticles has been observed.

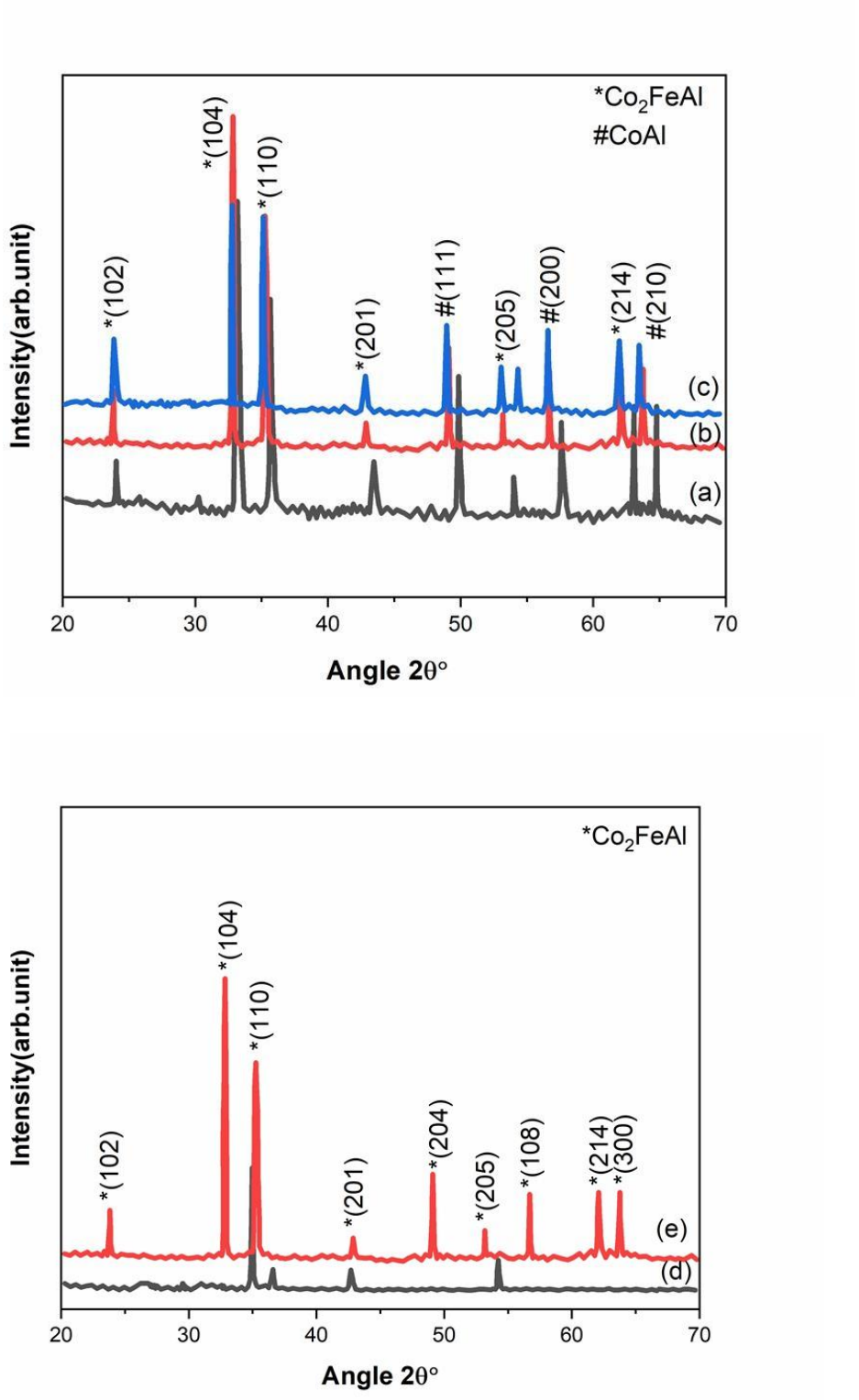

Figure 4.1 XRD patterns of Co2FeAl full Heusler alloys nanoparticles with respect to molarity (1.2, 1.4, 1.6, 1.8 and 2.0)

The crystallite size and dislocation density of Co2FeAl Full-Heusler Alloy can be evaluated by equation 4.1 and 4.2 (Cullity 1956).

$$t = \frac{0.9\,\lambda}{\beta cos\theta} \qquad (4.1)$$

$$\delta = \frac{1}{t^2} \qquad (4.2)$$

Where,

"t" is average crystallite size, "k" is the shape factor equal to 0.9, "λ" indicates wavelength (1.54050 Å) used in X-ray diffraction, "β" specifies the value of full width half maximum (FWHM) and "θ" is the Bragg's angle.

Fig 4.2 shows the crystallite size and dislocation density of Co_2FeAl full-Heusler Alloy nanoparticles with varying molarity from 1.2M to 2.0M. Initially the crystallite size increases from 1.2M to 1.6M due to the structural rearrangement. With further increase in molarity upto 1.8M, further increases in crystallite size is observed. Dislocation density shows the inverse behavior of crystallite size as shown in fig 4.2. The presence of dislocations and defects during the deposition process may be due to micro-strain present.[44].

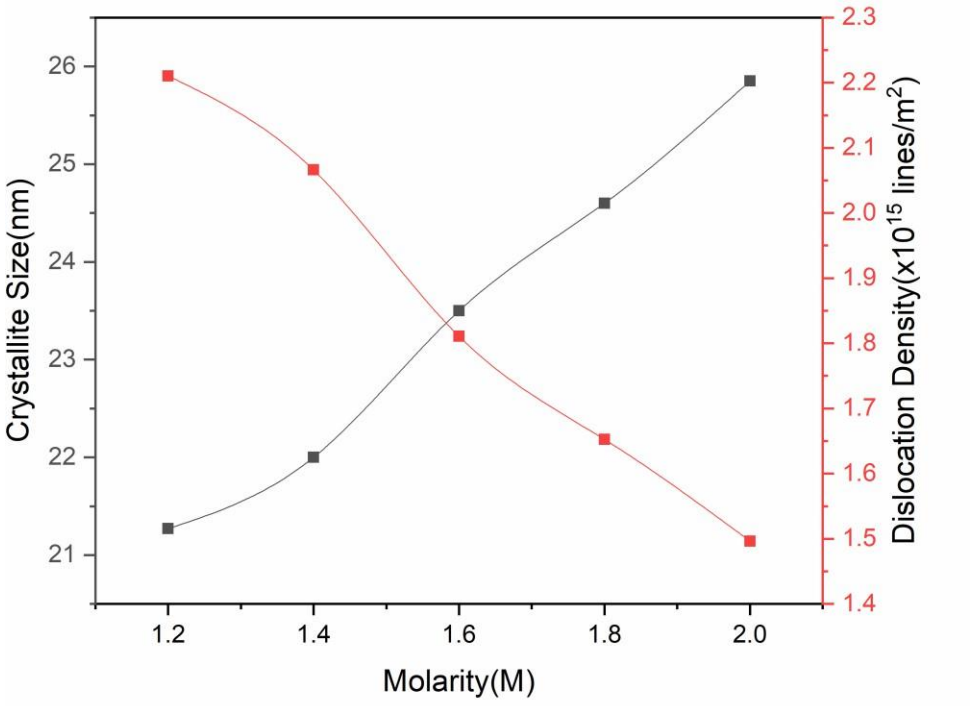

Figure 4.2 Variations in Crystallite size and Dislocation density of Co_2FeAl full Heusler alloys nanoparticles with respect to molarity (1.2, 1.4, 1.6, 1.8 and 2.0)

4.3 FTIR Analysis

FTIR spectroscopy is an importance for analyzing the micro-structural and vibrational behaviors of heusler alloy. In this method beam of infrared light interacts with the sample taken. The molecule then absorbs the energy when the vibration frequency of a chemical bond matches with the beam frequency. The wavelength whose absorption occurs is the characteristic of each type of covalent bond, enabling material characterization. The variation of FTIR spectrum with molarity is shown in Fig. 4.3. FTIR used to find out the functional groups in the sample. Bands related to alloy were not observed, however, band at 620 cm^{-1} represents C ≡C–H bending vibration mode, band at 1070 cm^{-1} represents C=O, band at 1434 cm^{-1} represents C-H and band at 1614 cm^{-1} shows O-H. The vibration bands at 2357 cm^{-1} were also assigned to CO_2 modes. The vibration around 3324 cm^{-1} indicated C ≡C–H stretching vibration mode of the water.

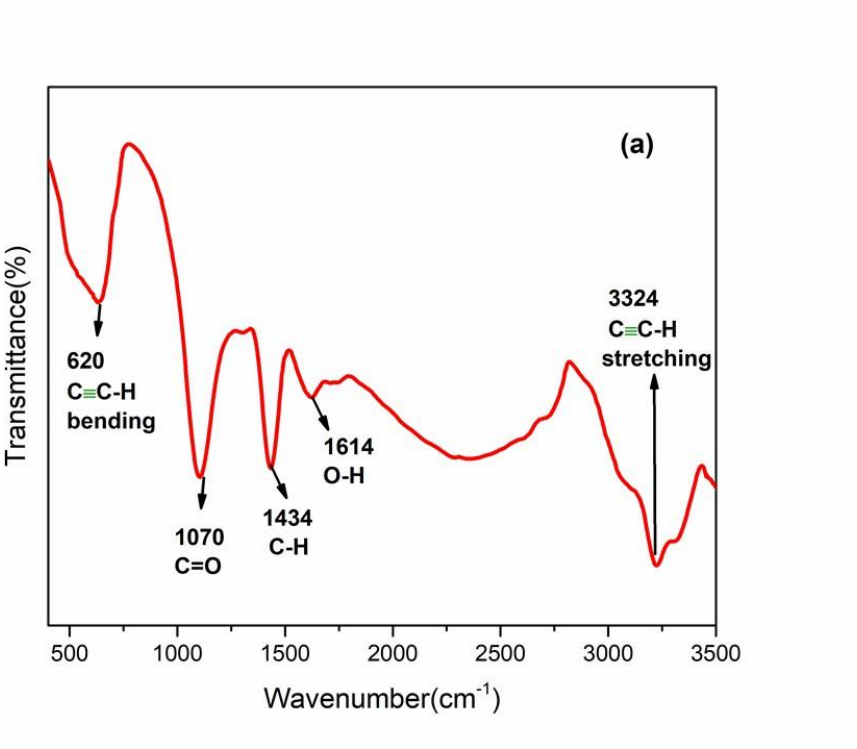

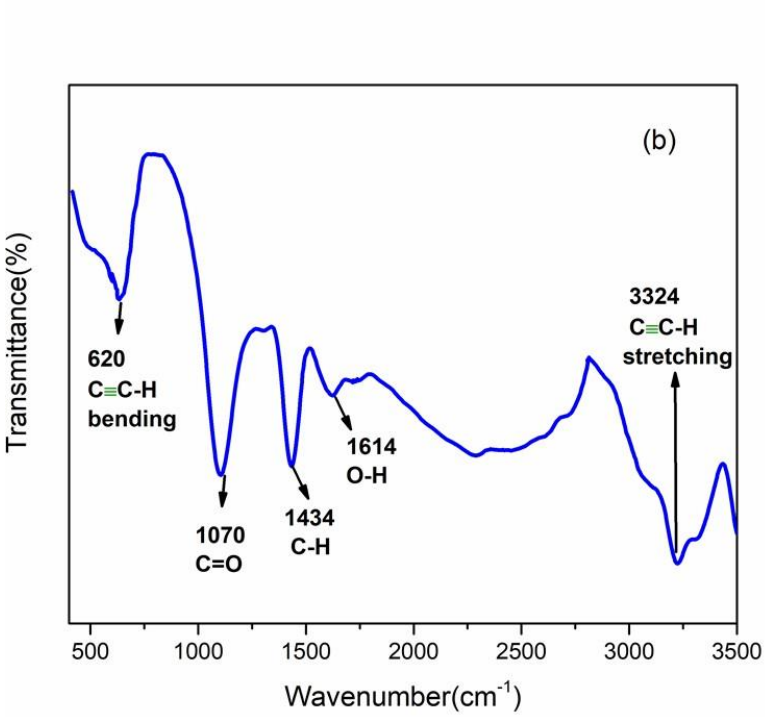
(b)
Transmittance(%)
620
C≡C-H
bending
1070
C=O
1434
C-H
1614
O-H
3324
C≡C-H
stretching
500
1000
1500
2000
2500
3000
3500
Wavenumber(cm-1)

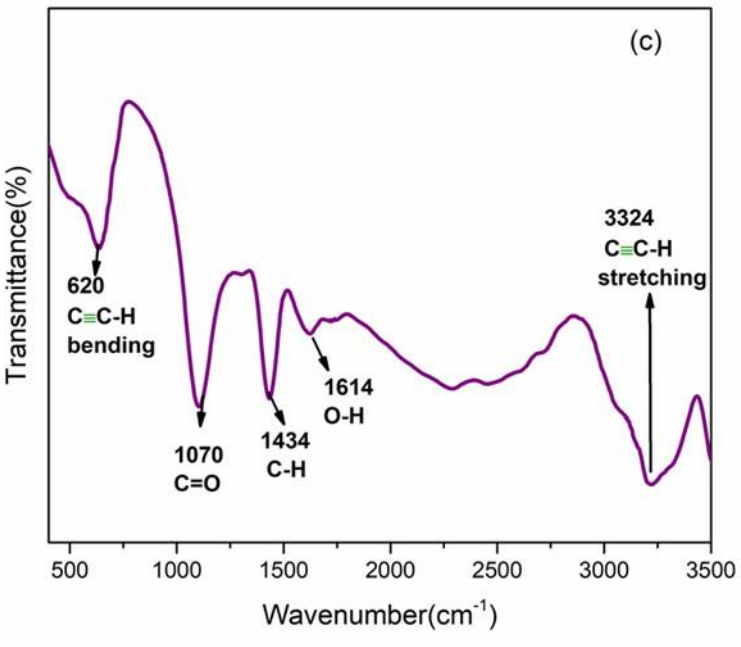
(c)
Transmittance(%)
620
C≡C-H
bending
1070
C=O
1434
C-H
1614
O-H
3324
C≡C-H
stretching
500
1000
1500
2000
2500
3000
3500
Wavenumber(cm-1)

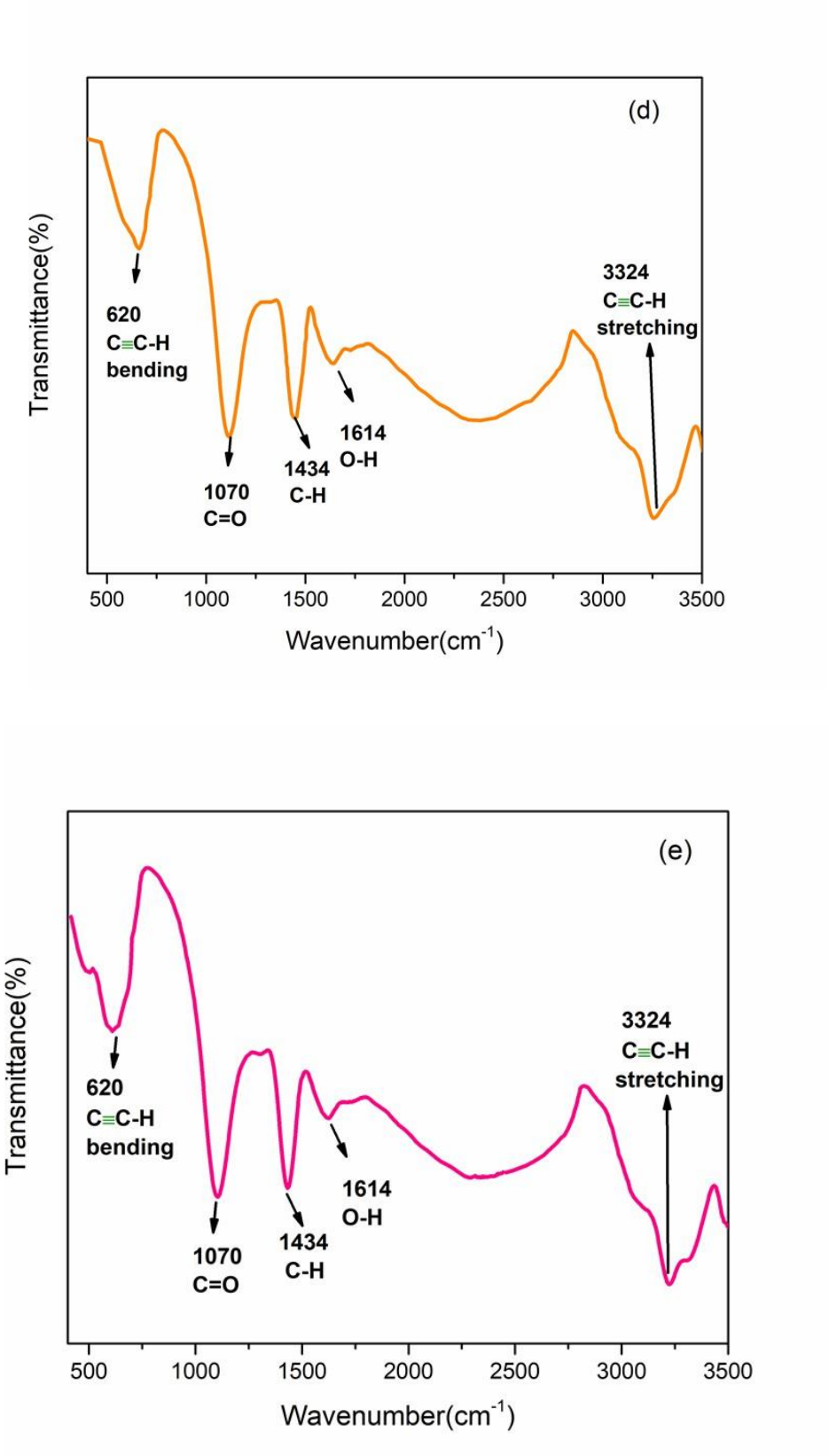

Figure 4.3 FTIR spectra of Co_2FeAl full Heusler alloys nanoparticles with respect to molarity (1.2, 1.4, 1.6, 1.8 and 2.0)

4.4 Magnetic Properties

Vibrating sample magnetometer (VSM) has used to evaluate the magnetic properties of Co_2FeAl full-heusler alloy. Fig 4.4 shows the magnetic hysteresis (M-H) loops for Co_2FeAl full-heuslar alloy nanoparticles with varying Molarity (1.2M to 2.0M) is shown, All the samples show the ferromagnetic behavior with low values of coercivity.

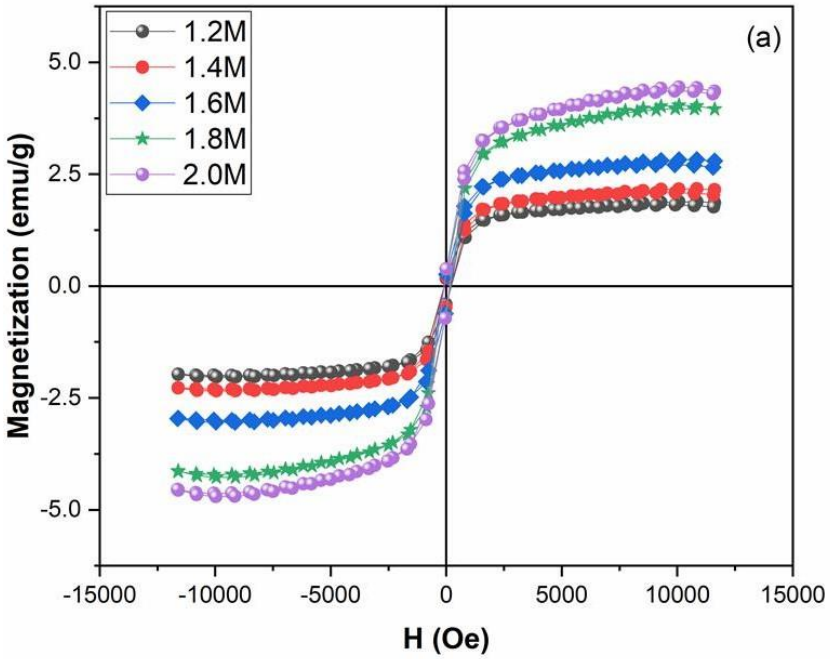

Figure 4.4 MH loops of Co_2FeAl full Heusler alloys nanoparticles with respect to molarity a) 1.2,

b) 1.4, c) 1.6, d) 1.8 and e) 2.0

In Fig 4.5 it is shown that the saturation magnetization of Co_2FeAl full-heuslar alloy nanoparticles with varying Molarity (1.2M-2.0M). The values of M_S has been plotted for all Co_2FeAl based Heusler alloy nanoparticles with varying Molarity (1.2M to 2.0M). The saturation magnetization values increase from 1.2M to 2M due to increasing crystallinity and crystallite size. The lowest value of saturation magnetization observed at 1.2M is 0.003emu/g and the highest value of saturation magnetization observed at 2M is 0.0087emu/g.

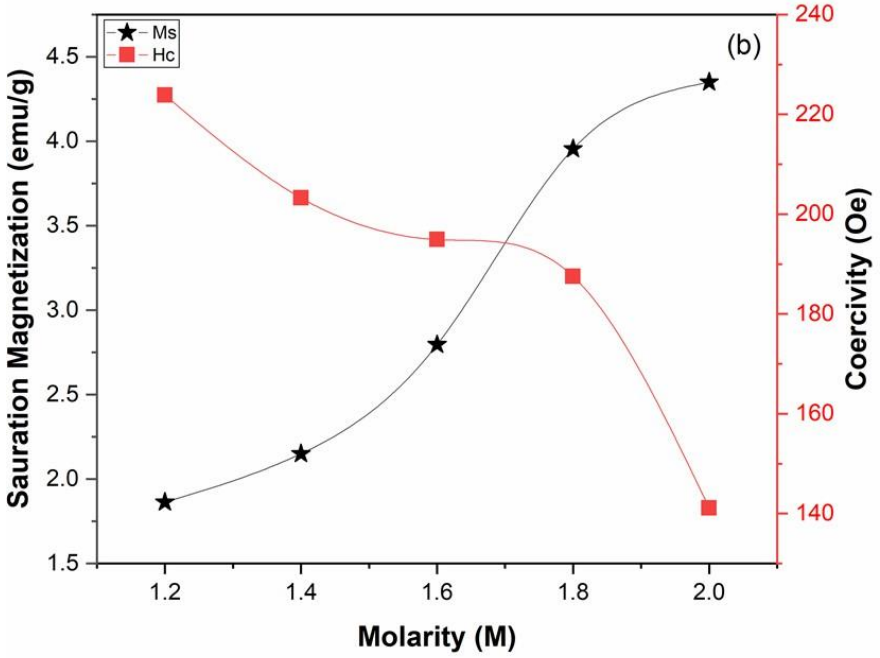

Figure 4.5 Saturation Magnetization and Coercivity curves of Co_2FeAl full Heusler alloys nanoparticles with respect to molarity 1.2, 1.4, 1.6, 1.8 and 2.0

4.5 Mechanical Strength

The hardness of full heuslar alloy Co2FeSn at various molarities 1.2 M, 1.4 M, 1.6 M, 1.8 M, 2.0 M) alloy was determined through Shimadzu hardness HMV-2 Vickers micro indenter by applying Vickers indenter for 15 seconds at load of 4.903 N as recommended by ASTM C1327-99. Figure 4.6 shows high hardness values (~8.08-8.93 GPa) for the samples prepared at molairty of 1.8-2.0 due to pure phase formation and stabilization with increase in molarity are observed.Whereas, lower values of hardness (~5.83 -7.23 GPa), in low malorities, are due to the presence of mixed crystal phases as discussed in XRD results [Fig. XRD].

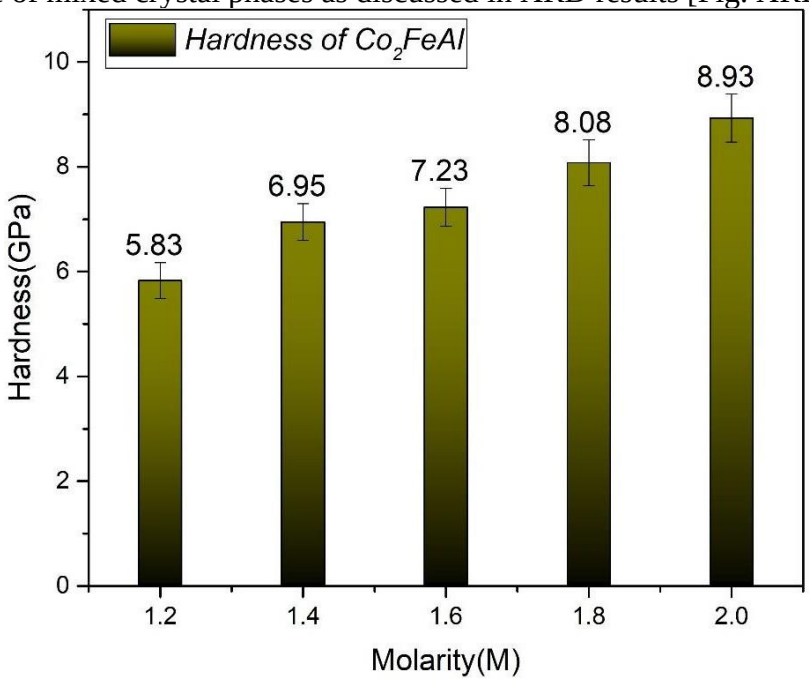

Figure 4.6 Hardness values of Co2FeAl alloy at different molarities (1.2, 1.4, 1.6, 1.8 and 2.0)

4.6 I-V Characteristics

Figure 4.7 shows typical I-V characteristics of a Co2FeAl full Heusler alloys for the samples prepared with varying molarity i.e. 1.2M to 2.0M. The I-V characteristics shows linear characteristics and were almost symmetric with respect to the bias polarity, which indicated that the conduction was dominant. However, a slightly larger current was obtained for the forward bias, which was probably due to a thermionic emission current through interface for the forward bias. Figure 4.8 shows the I-V characteristics at various temperatures (T) measured by three-terminal geometry. The IV curves showed linear characteristics and all of them are almost symmetric with bias. The I-V characteristics were slightly dependent on temperature.

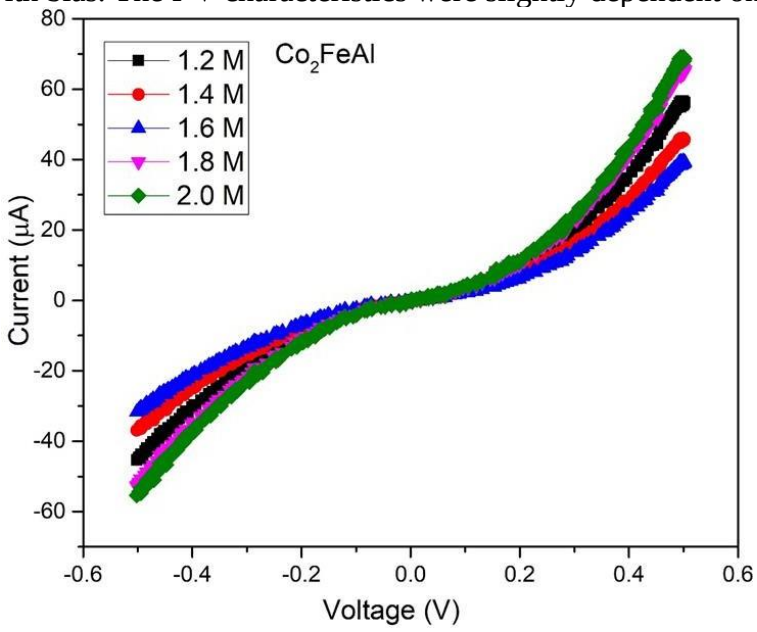

Figure 4.7 I-V characteristics of Co2FeAl alloy at different molarities (1.2, 1.4, 1.6, 1.8 and 2.0)

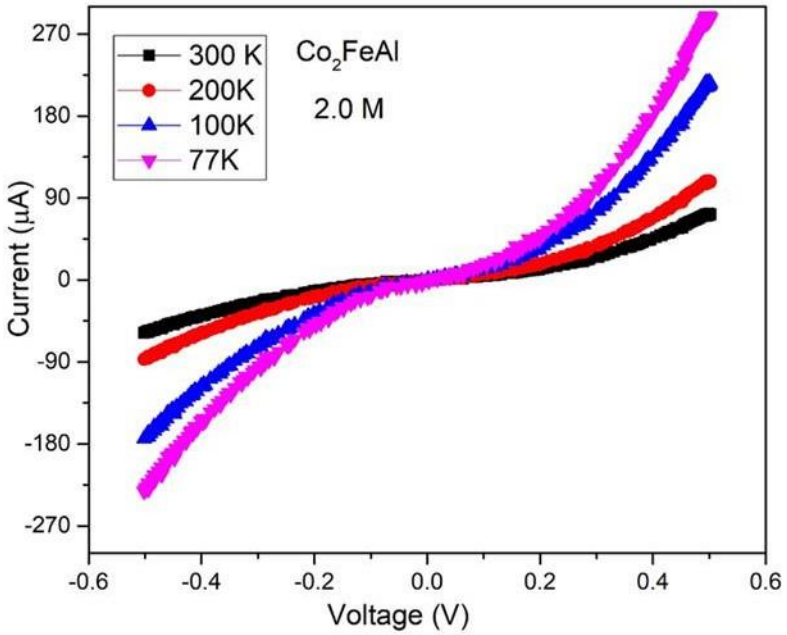

Figure 4.8 Temperature dependent I-V characteristics of Co2FeAl alloy

Conclusions

In the present study, the Co2FeAl full-heuslar alloy nanoparticles were prepared by hydrothermal method. Pure Co2FeAl -hexagonal phase was observed at 1.8M and 2.0M of molarity. The crystallite size of Co2FeAl full-heuslar alloy nanoparticles was observed in the range of 21nm to 26nm. FTIR spectra showed C≡C-H, acetylene and monosubstitute alkynes show characteristically strong absorption at 620 cm^{-1} region due to C-H bending vibrations and also C≡C-H mono substituted alkynes are easily characterized by a strong broad absorption band 3324 cm^{-1} arising from the C≡C-H stretching vibrations. The M-H Loops of the Co2FeAl Alloys showed the soft ferromagnetic behavior with high value of saturation magnetization (~4 emu/g) for the optimized sample. Maximum condution was observed for the phase pure sample. Increase in condution mechanism was observed with decrease in temperature.

References

1. Mody, V. V., Siwale, R., Singh, A., & Mody, H. R. (2010). Introduction to metallic nanoparticles. *Journal of Pharmacy and Bioallied Sciences*, *2*(4), 282.
2. Felser, C., & Hirohata, A. (2015). *Heusler alloys* (p. 10). Berlin: Springer.
3. Inomata, K., Okamura, S., Goto, R., & Tezuka, N. (2003). Large tunneling magnetoresistance at room temperature using a Heusler alloy with the B2 structure. *Japanese journal of applied physics*, *42*(4B), L419.
4. Yin, M., Hasier, J., & Nash, P. (2016). A review of phase equilibria in Heusler alloy systems containing Fe, Co or Ni. *Journal of materials science*, *51*(1), 50-70.
5. Liu, Z. H., Zhang, M., Wang, W. Q., Wang, W. H., Chen, J. L., Wu, G. H., ... & Li, Y. X. (2002). Magnetic properties and martensitic transformation in quaternary Heusler alloy of NiMnFeGa. *Journal of Applied Physics*, *92*(9), 5006-5010.
6. Hou, C. K., Hu, C. T., & Lee, S. (1991). The effect of aluminium on the magnetic properties of lamination steels. *IEEE transactions on magnetics*, *27*(5), 4305-4309.
7. Wójcik, M., Jedryka, E., Sukegawa, H., Nakatani, T., & Inomata, K. (2012). 59 Co NMR experiment as a probe of electron doping in Co 2 FeAl 1− x Si x Heusler alloys. *Physical Review B*, *85*(10), 100401.
8. Ortiz, F. (2019). *The Cuban Counterpoint* (pp. 222-226). Duke University Press.
9. Feichtinger, H. G., & Strohmer, T. (Eds.). (2012). *Gabor analysis and algorithms: Theory and applications*. Springer Science & Business Media.
10. De Groot, S. R., & De Groot, S. R. (1951). *Thermodynamics of irreversible processes* (Vol. 242). Amsterdam: North-Holland.
11. Okamura, H., Tsutsui, H., Komatsu, T., Yutsudo, M., Hakura, A., Tanimoto, T., ... & Kurimoto, M. (1995). Cloning of a new cytokine that induces IFN-γ production by T cells. *Nature*, *378*(6552), 88-91.
12. Qu, D., Zheng, M., Du, P., Zhou, Y., Zhang, L., Li, D., ... & Sun, Z. (2013). Highly luminescent S, N co-doped graphene quantum dots with broad visible absorption bands for visible light photocatalysts. *Nanoscale*, *5*(24), 12272-12277.
13. Qu, D., Zheng, M., Du, P., Zhou, Y., Zhang, L., Li, D., ... & Sun, Z. (2013). Highly luminescent S, N co-doped graphene quantum dots with broad visible absorption bands for visible light photocatalysts. *Nanoscale*, *5*(24), 12272-12277.
14. Bhandari, M., Devereaux, P. J., Tornetta III, P., Swiontkowski, M. F., Berry, D. J., Haidukewych, G., ... & Guyatt, G. H. (2005). Operative management of displaced femoral neck fractures in elderly patients: an international survey. *JBJS*, *87*(9), 2122- 2130.
15. Li, D., Chen, X., Zhang, Z., & Huang, K. (2017). Learning deep context-aware features over body and latent parts for person re-identification. In *Proceedings of the IEEE conference on computer vision and pattern recognition* (pp. 384-393).
16. Isharma, I. (2016). I, i SHARMA.
17. Kumar, R. (2021). H KUMAR.
18. Vivek, S. D., Beatty, S. E., Dalela, V., & Morgan, R. M. (2014). A generalized

multidimensional scale for measuring customer engagement. *Journal of Marketing Theory and Practice*, *22*(4), 401-420.
19. Schmid, P., Adams, S., Rugo, H. S., Schneeweiss, A., Barrios, C. H., Iwata, H., ... & Emens, L. A. (2018). Atezolizumab and nab-paclitaxel in advanced triple-negative breast cancer. *New England Journal of Medicine*, *379*(22), 2108-2121.
20. Wang, X. A., & Wang, X. Y. (2007). Design of a Kind of Pocket Electronic Balance [J]. *Light Industry Machinery*, *2*.
21. Wang, X. A., & Wang, X. Y. (2007). Design of a Kind of Pocket Electronic Balance [J]. *Light Industry Machinery*, *2*.
22. . Lujaji, F. C., Boateng, A. A., Schaffer, M. A., Mullen, C. A., Mkilaha, I. S., & Mtui, P. L. (2016). Pyrolysis oil combustion in a horizontal box furnace with an externally mixed nozzle. *Energy & Fuels*, *30*(5), 4126-4136.
23. . Lujaji, F. C., Boateng, A. A., Schaffer, M. A., Mullen, C. A., Mkilaha, I. S., & Mtui, P. L. (2016). Pyrolysis oil combustion in a horizontal box furnace with an externally mixed nozzle. *Energy & Fuels*, *30*(5), 4126-4136.
24. Adya, A., Dunagan, J., & Wolman, A. (2010, April). Centrifuge: Integrated Lease Management and Partitioning for Cloud Services. In *NSDI* (Vol. 10, pp. 1-16).
25. Tam, K. H., Cheung, C. K., Leung, Y. H., Djurišić, A. B., Ling, C. C., Beling, C. D., ... & Ge, W. K. (2006). Defects in ZnO nanorods prepared by a hydrothermal method. *The Journal of Physical Chemistry B*, *110*(42), 20865-20871.
26. Tam, K. H., Cheung, C. K., Leung, Y. H., Djurišić, A. B., Ling, C. C., Beling, C. D., ... & Ge, W. K. (2006). Defects in ZnO nanorods prepared by a hydrothermal method. *The Journal of Physical Chemistry B*, *110*(42), 20865-20871.
27. Straumanis, M. E. (1949). The precision determination of lattice constants by the powder \and rotating crystal methods and applications. *Journal of Applied Physics*, *20*(8), 726- 734.
28. Sodhi, G. S., & Kaur, J. (2001). Powder method for detecting latent fingerprints: a review. *Forensic science international*, *120*(3), 172-176.
29. Sodhi, G. S., & Kaur, J. (2001). Powder method for detecting latent fingerprints: a review. *Forensic science international*, *120*(3), 172-176.
30. Werner, F. (2017). Hall measurements on low-mobility thin films. *Journal of Applied Physics*, *122*(13), 135306.
31. Riaz, T., Zeeshan, R., Zarif, F., Ilyas, K., Muhammad, N., Safi, S. Z., & Rehman, I. U. (2018). FTIR analysis of natural and synthetic collagen. *Applied Spectroscopy Reviews*, *53*(9), 703-746.